

Final Report Certification
for
CRADA Number 0708

ENTERED
IPM
10-9-08
RCS

Between

UT-Battelle, LLC

and

American Superconductor Corporation
(Participant)

Instructions:

Mark the appropriate statement in 1a or 1b below with an 'IX.' Refer to the articles in the CRADA terms and conditions governing the identification and marking of Protected CRADA Information (PCI).

If no PCI is identified, the report will be distributed without restriction. If PCI is identified, the report distribution will be limited in accordance with the CRADA terms and conditions governing release of data. In all cases items 2 and 3 must be true. That is, the report cannot contain Proprietary Information and a disclosure must be filed prior to release of the report.

This certification may either be made by using this form or may be made on company letterhead if the Participant desires. A faxed copy of this completed form is acceptable.

The following certification is made for the subject final report:

1. (a) ☐ The final report contains information that qualifies as "Protected CRADA Information" (PCI). The PCI legend is printed on the report cover, and the PCI is clearly identified.

OR

- (b) ☒ The final report does not contain "Protected CRADA Information." The "Approved for Public Release" legend is printed on the report cover.

2. The final report does not contain Proprietary Information.
3. By the signature below, the Participant has no objection to the public distribution of the final report due to patentable information.

For the Participant:

Martin Riquel
(Name)

Senior Technical manager
(Title)

08/08/2008
(Date)



Contract No. W31P4Q-05-C-R033

Defense Advanced Research Projects Agency (DOD)

DARPA Order S039-08

Issued by U. S. Army Aviation and Missile Command Under

"LOW COST FABRICATION OF 2G WIRES FOR AC APPLICATIONS"

Final Report

September 19, 2005

Prepared by:
Dr. Thomas Kodenkandath
American Superconductor Corporation
Westborough, MA 01581

And

Dr. Fred List
Oak Ridge National Laboratory
Oak Ridge, TN 37831

Approved for Public Release

Table of Contents

EXECUTIVE SUMMARY	3
INTRODUCTION and OVERVIEW	3
Project Objectives	3
Technical Approach	3
PHASE I RESULTS	4
Task 1: Fabrication and Demonstration of an Inkjet Printer for YBCO Films	4
Task 2: Printing, Processing and Characterization of YBCO Filament	7
Task 3. Optimization and Characterization of Inkjet Patterned YBCO Films	8
Task 3-a. Additional Task beyond Phase I SOW	17
Task 4. Commercial Inkjet Design and Assessment.	19
REFERENCES	23

EXECUTIVE SUMMARY

Ink-jet printing has been demonstrated as an adaptable technology for printing YBCO filaments using a Metal Organic (MO) YBCO precursor. The technology was demonstrated using AMSC's proprietary metal organic TFA-based YBCO precursor and a commercial piezoelectric print-head on RABiTS templates. Filaments with a width of 100 μm and spacing of 200 μm were successfully printed, decomposed and processed to YBCO. Critical currents of $\sim 200 \text{ A/cm-w}$ were achieved in a series of filaments with a 2 mm width. The single nozzle laboratory printer used in the Phase I program is capable of printing $\sim 100 \mu\text{m}$ wide single filaments at a rate of 8-10 cm/sec. The electrical stabilization of filaments with a Ag ink was also evaluated using ink-jet printing.

INTRODUCTION and OVERVIEW

Project Objectives

The overall objective of the Phase I Project was the evaluation and demonstration of inkjet-printing for depositing YBCO filaments on textured templates (RABiTS, IBAD, ISD, etc substrates) with properties appropriate for low loss ac conductors. Goals of the Phase I program included development of an appropriate precursor ink, demonstration of the printing process, processing and characterization of printed YBCO filaments and evaluation of the process for further development.

Technical Approach

The incorporation of second generation (2G) superconducting YBCO wires into HTS motors, transformers, inductors or generators provides the opportunity to dramatically reduce device cooling requirements, thus enabling the development of lightweight, compact, high-power devices for a variety of military and commercial applications. One of the major advantages of the 2G wire is the potential to develop conductor architectures with drastically reduced ac losses compared to first generation (1G) BSCCO/Ag composite HTS wires [1, 2]. AMSC has demonstrated the fabrication of 2G wires in lengths of 85 meters with critical currents up to 168 A/cm-w (77K, self-field) [3,4,5]. AMSC's manufacturing process is based on combining low cost metal organic deposition (MOD) of the YBCO layer with a RABiTSTM-type template [4,6,7,8,9,10]. The performance of these 2G wires is approaching that required for commercial applications. Although 2G wire is suitable for many types of electric power devices, including motors and power transmission cables, the ac losses from the wide YBCO

conducting layers are too high for use in the synchronous generator armature windings and compact transformers of interest for military applications.

It has been established that dividing a YBCO film into thin filament arrays can significantly suppress the ac loss of $\text{YBa}_2\text{Cu}_3\text{O}_7$ (YBCO) coated conductor [11,12,13]. However, this approach lowers the effective current density of the whole wire due to the concomitant reduction of the HTS material within the wire. Therefore, the structure of the electrical wire must be optimized to obtain large critical currents with minimized ac loss.

There are many potential ways to narrow the width of coated conductors to achieve the required structure shown in Figure 1; however, no standard method has been demonstrated that is applicable to *low-cost* manufacturing of practical conductors. One of the requirements of the processing is the need to form the superconducting layer precisely with gaps ideally less than fifty microns wide, to remove the material from the substrate cleanly, and not to damage the remaining active filaments during the processing. The general approaches previously used for this work have been laser ablation or photolithography/chemical etching; however, such processing is expensive, and there are attendant concerns that re-deposition of the removed YBCO and thermal or chemical damage to the residual filaments can cause degradation of the critical temperature and critical current density of the film. In addition, both of these processes remove a significant fraction of the YBCO layer, adding to the cost of the overall conductor.

This program focused on evaluating Ink Jet Printing as a new method for forming thin filament arrays that span the entire width of a coated conductor tape.

PHASE I RESULTS

Task 1: Fabrication and Demonstration of an Inkjet Printer for YBCO Films

Commercial piezoelectric inkjet printers (Epson) were initially evaluated for use in the program. However, it was established that the characteristics of the Metal Organic precursor ink were not compatible with the "off the shelf" piezoelectric print heads used in standard printers. The major problem was in properly modifying the "off the shelf unit" to accept the precursor ink with out leaking from the print head nozzle during the set up. In addition, the speed at which the print head could be positioned was not rapid enough to prevent drying of the ink in the printer head nozzle. Thus a number of inkjet printer manufactures were evaluated for their ability to carry out the initial printing trials. After evaluating a number of

potential vendors, MicroFab Technologies, Inc. of Plano, TX was selected to carry out the initial trials.

The printing trials during the Phase I program were all carried out using a single nozzle, 55 μm piezoelectric print head. The basic configuration of the piezoelectric print head is illustrated in Figure 1. In this type of print head, the piezoelectric elements are deformed by electrical pulses causing ink droplets to be ejected. The deformation of piezoelectric elements puts pressure on the ink chamber through the intermediary of flexible substances, which generates ink ejection energy.

The print head was mounted to a precision x-y stage ($\pm 10\mu\text{m}$ accuracy) and the substrates were mounted on a vacuum table under the print head. The printing was controlled through a computer interface.

Figure 2 shows the printing set up used during the Phase I program. Printing enclosure was vented to remove any solvents; however, the atmosphere over the substrate surface could not be controlled separately from the room environment.

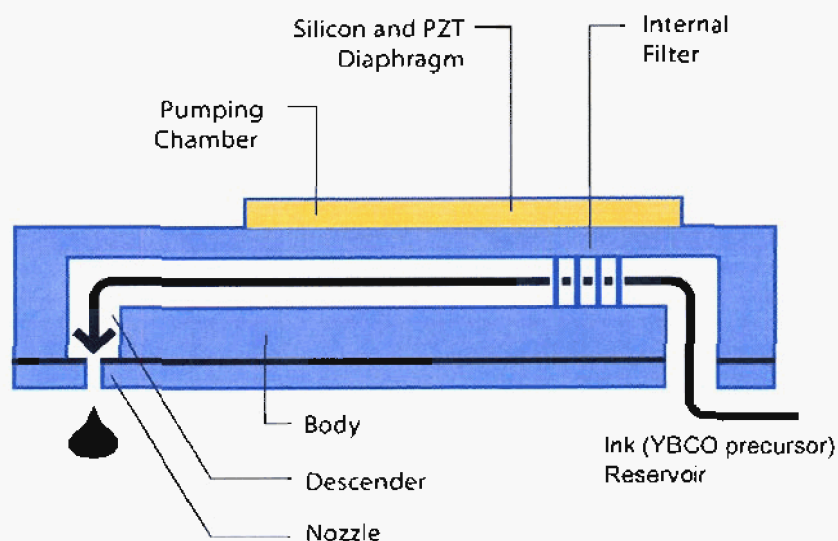


Fig. 1. Schematic of a typical piezoelectric type print head used on the Phase I program.

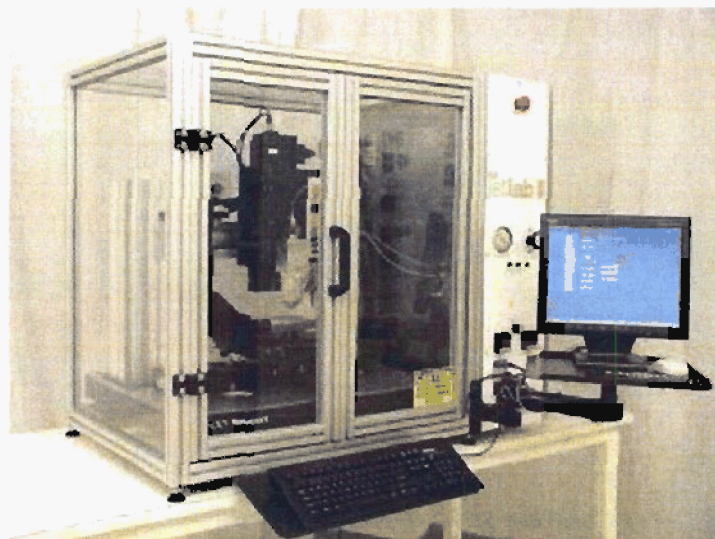


Fig. 2. Photograph of the ink jet printer and controller (located at MicroFab Technologies, Inc.) used during the Phase I program.

Various properties of the ink (i.e., the viscosity, the solid loading, solvent evaporation rate, etc.) must be optimized to insure that individual droplets can be ejected in the form of droplets from nozzles with a diameter of less than 100 micrometers.

The initial printing trials focused on characterizing the precursor ink and establishing its compatibility with the piezoelectric print head. A proprietary ink was developed at AMSC that was compatible with the piezoelectric print head. Testing at the MicroFab facility allowed additional optimization of the jettability of the precursor ink. Figure 3 shows the typical droplet formation of an optimized ink formulation and the dimensions of the as printed individual droplets on the substrate. The droplets remained intact during subsequent decomposition process (which involves the thermal burn out of the organic components of the precursor film). The modified ink also wetted the substrate well. The reformulated precursor ink was also tested in AMSC's standard coating process to confirm that the same performance (critical current) was achieved. The results showed there was no difference between the standard and reformulated ink.

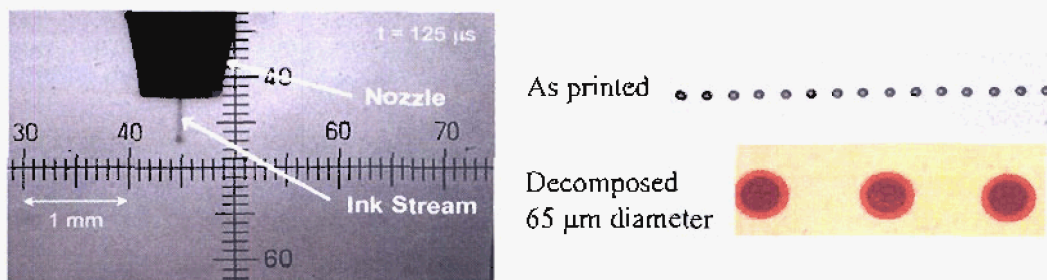


Fig. 3. (A) Image of the precursor ink drop ejected from the 55 μm piezoelectric nozzle; (B) pattern of individual ink droplets placed along substrate and (C) magnified image of the individual droplets after thermal removal of the organic components of the ink. Diameter of decomposed droplet is $\sim 65 \mu m$.

Task 2: Printing, Processing and Characterization of YBCO Filament

Using the printing parameters and reformulated precursor ink developed in Task 1, a series of parallel stripes were printed to establish the coverage and dimensional uniformity of the printed pattern. Printing parameters (droplet size, droplet overlay, ink formulation, etc.) were optimized to produce a final YBCO film thickness of nominally 0.8 μm thickness. Figure 4 shows an "as-printed" coating with a width of 1 mm. Imaging of the "as printed" line shows complete coverage, uniform width dimension with well defined edges. Although the droplet size and therefore the minimum line width can be adjusted by altering the nozzle diameter and ink properties, this was not examined in the Phase I program.

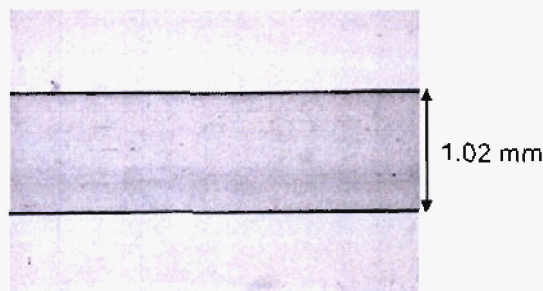


Fig. 4. Optical image of a 1 mm wide "as printed" YBCO filament on a RABiTS template.

Initial filaments printed at MicroFab were shipped to AMSC for subsequent processing and testing. The samples were decomposed using the standard process developed at AMSC.

Processing of patterned YBCO films was initially tested by mechanically scribing a standard 0.8 μm YBCO film deposited on a RABiTS substrate. The YBCO precursor film was striated

into ~200 μm wide lines as shown in Figure 5. The film was then processed to the superconducting YBCO film. Characterization of the processed filaments confirmed that the striated filaments can be converted to the YBCO using the standard technique used for un-patterned YBCO films. Critical current measurements of the striated YBCO film showed the expected A/cm-width values. No measurements were carried out on the individual filaments.

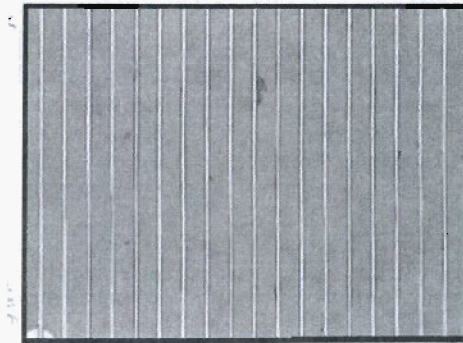


Fig. 5. Optical images of mechanically striated YBCO precursor films. Filament widths are approximately 200 μm .

Ink jet printed samples were processed as ~1 – 2 cm lengths using the standard short sample techniques developed for the conventional samples. Typical processing of the samples showed the formation of well textured YBCO as shown in Figure 5.

Task 3. Optimization and Characterization of Inkjet Patterned YBCO Films.

Once the basic printing parameters were established, experiments were carried out to demonstrate the ability to print filaments with varying widths, varying interline spacing and varying thickness. In the first round of experiments several patterns of YBCO filaments were printed to demonstrate the potential of the technology with respect to filament width and spacing.

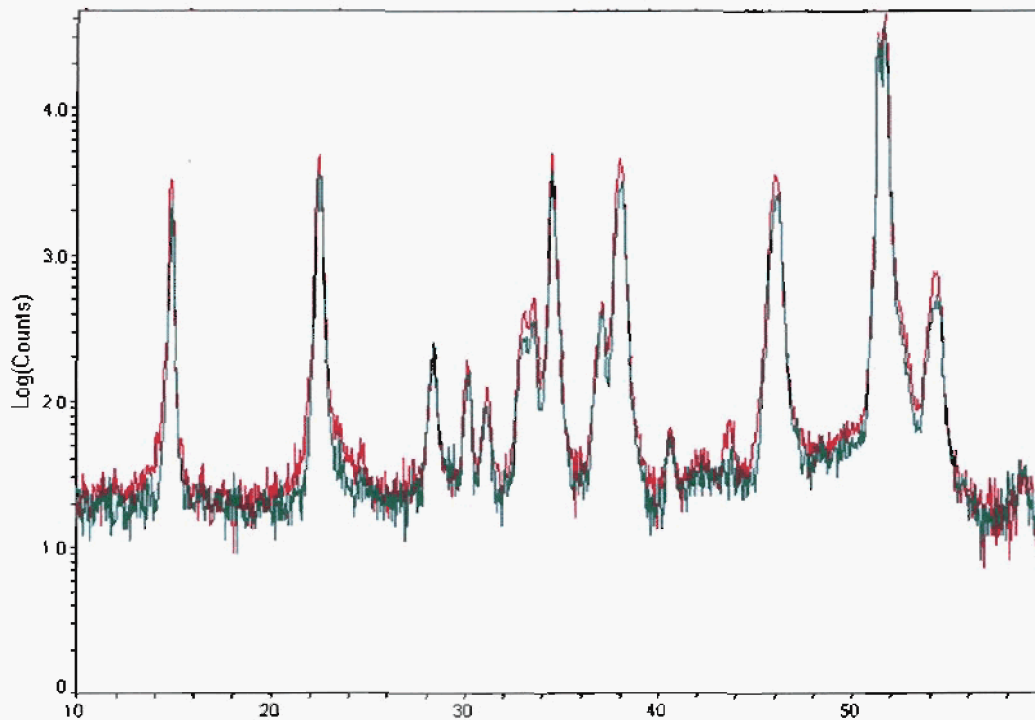


Fig. 5. X-ray diffraction pattern (Θ - 2Θ) of two different filamentized YBCO tapes prepared by ink jet printing showing the formation of c-axis textured YBCO in the ink jet printed films. The two patterns are superimposed and nearly identical.

Filament Width Demonstration. Figure 7 shows a series of “as printed” and decomposed filaments with widths from 100 μm to 2 mm. The filaments were printed with multi-passes of the print head with a 50 μm offset between each pass. This resulted in an overlap of ~ 15 μm for each droplet. Thus the 100 μm filament was printed with two passes and the 2 mm filament was printed with 40 passes. The linear spacing between droplets was also set at 50 μm . This resulted in complete coverage across the width of the filaments and well defined filament widths.

After decomposition of the filaments, the width and dimensions were virtually unchanged as seen in Figure 7.

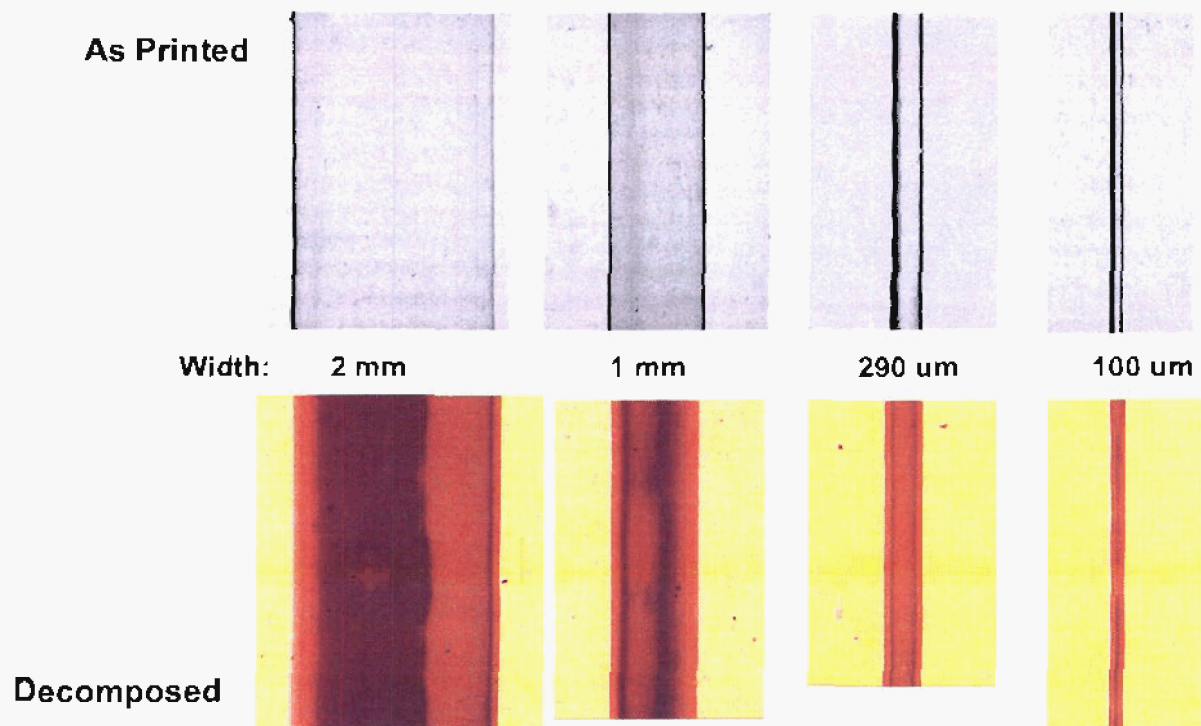


Fig. 7. Images of the "as printed" and decomposed filaments printed at widths of 2 mm to 100 μm .

Filament Spacing Demonstration. Figure 8 shows a series of ~ 125 μm wide filaments printed with an interfilament spacing of 375, 175 and 75 μm . Figure 9 shows that the filaments integrity, dimensions and interfilament spacing are retained with no change through the decomposition and YBCO reaction processes.

The results also demonstrated that a minimum interfilament spacing of at least 75 μm was readily achievable without any evidence of filament merging through the printing and subsequent processing steps as shown in Figure 10,

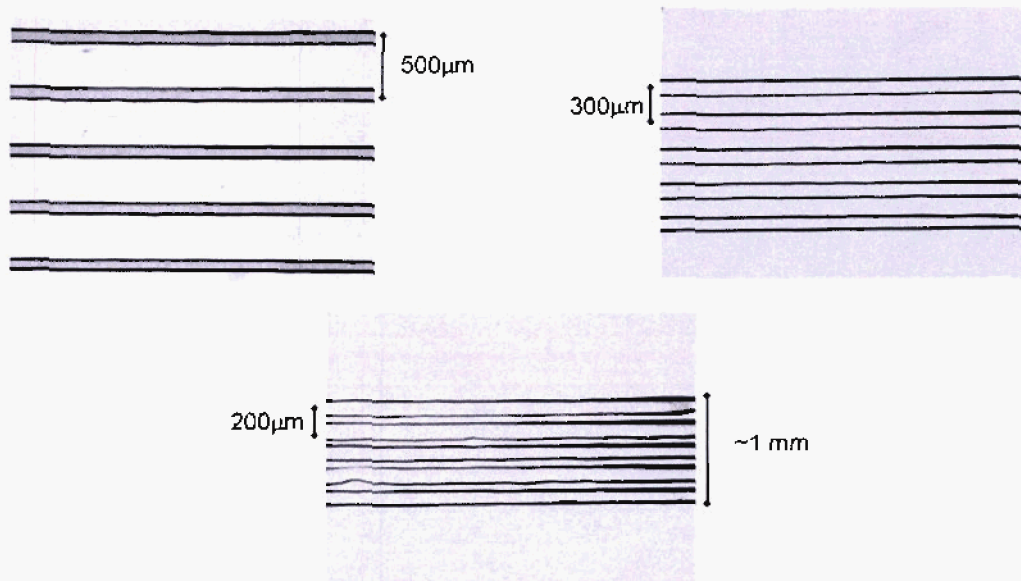


Fig. 8. Images of the "as printed" and decomposed filaments printed at widths of 2 mm to 100 μm .

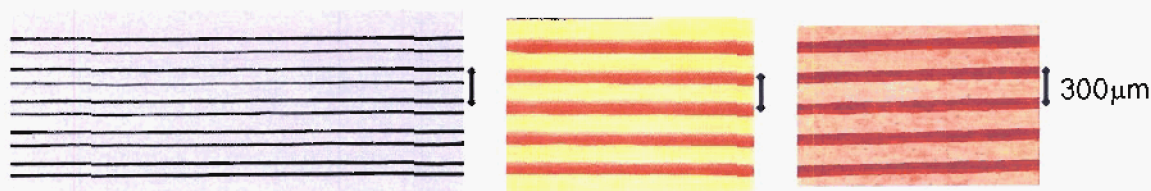


Fig. 9. Images of "as printed", decomposed and reacted YBCO filaments with a filament width of 125 μm and interfilament spacing of 175 μm .

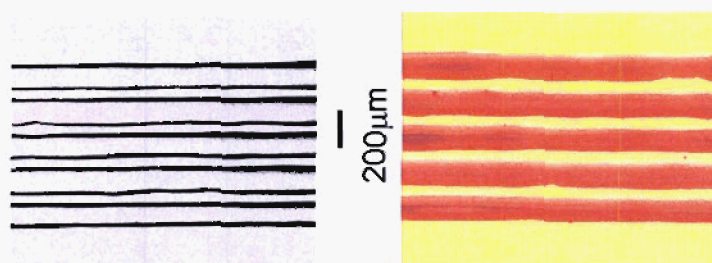


Fig. 10. Images of "as printed" and decomposed YBCO filaments with a filament width of 125 μm and interfilament spacing of 75 μm .

Filament Thickness Demonstration. The thickness of the YBCO filament is determined by the droplet volume, the solution viscosity, substrate wettability, the metal concentration in the

precursor ink and the droplet overlap. Figure 10 shows that as the metal concentration in the precursor ink decreases, the droplet spreads more as it impacts the substrate and the thickness of the coating decreases. Thus by varying the precursor ink properties along with the droplet placement it is possible to control the filament thickness,

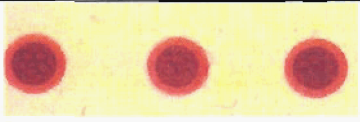
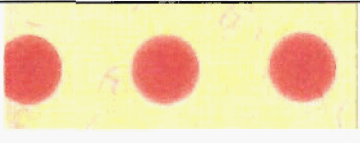
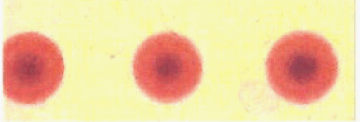
Ink Concentration	Diameter (μm)	Thickness (μm)	Decomposed Droplet Image
High	65	2.7	
Medium	75	1.9	
Low	90	1.1	

Fig. 10. Thickness and diameter of individual ink jet droplets, after decomposition, as a function of the metal concentration of the precursor ink.

The initial filament thickness during the Phase I test was targeted at $0.8\ \mu\text{m}$ (final YBCO thickness). TEM cross-sectional imaging of a fully processed YBCO filament, in Figure 11, showed that actual thickness is $0.8\ \mu\text{m}$ which is the targeted filament thickness.

A series of $\sim 200\ \mu\text{m}$ wide filaments were printed with a targeted thickness of 1.6 and $2.4\ \mu\text{m}$ YBCO using a multi-pass technique. Although the ink jet process was able to successfully deposit the thicker filaments, there was cracking observed during the decomposition process as shown for the $1.6\ \mu\text{m}$ thick YBCO filaments in Figure 12. Due to the limited number of thicker YBCO samples prepared, it was not possible to optimize the decomposition process during the Phase I program.

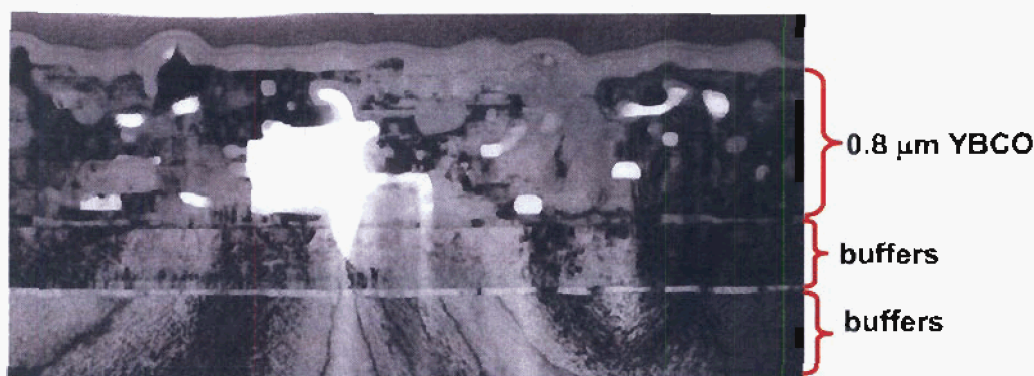


Fig. 11. TEM cross-section showing thickness of YBCO filament. Target thickness was 0.8 μm.

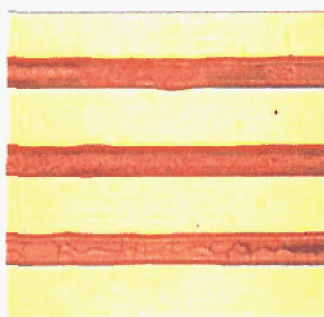


Fig. 12. Optical micrograph of ink jet printed, 1.6 μm thick YBCO filaments, showing cracking that occurred during the decomposition process. Filament width was ~ 200 μm.

Electrical Characterization. Processing of the ink jet printed filaments to the YBCO phase was carried out using the standard short process developed for the full width (1 - 4 cm) YBCO films. The reaction process, shown in equation 1,



is dependent on the equilibrium $[\text{HF}_g]$ concentration over the surface of the film during the high temperature processing. Figure 13 shows the I_c -V curve for a 2 mm wide YBCO filament. The measured I_c across the 4 filaments corresponds to an I_c (A/cm-width) equivalent to ~ 200 A/cm-width. This is typical of the I_c 's obtained with full width YBCO films of the same thickness on the same substrate.

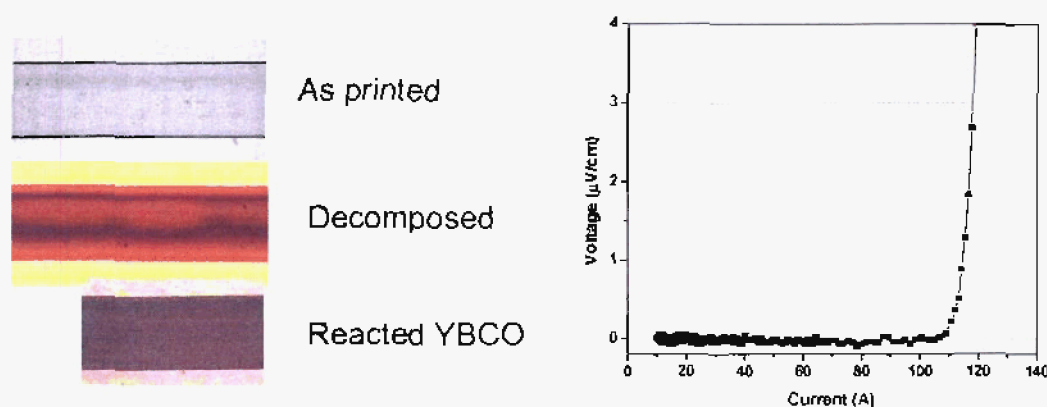


Fig. 13. I-V curve for a 2 mm wide YBCO filaments (0.8 μm thick) prepared by ink jet printing on a RABiTS substrate. The measured I_c corresponds to $\sim 200 \text{ A/cm-width}$.

Interconnected Filaments. A series of parallel filaments were printed to demonstrate the ability to use the ink jet printing to prepare interconnected filaments. The Interconnections were prepared by initially printing the parallel filaments, then in a second pass, the interconnects between filaments were deposited. The interconnects were printed with a partial overlap of parallel filaments as shown in Figure 14. As seen in Figure 14, the overlap, which resulted in a region of the filament with a thickness of $\sim 1.6 \mu\text{m}$ showed cracking during the decomposition. This is the same behavior observed with the thick filaments described above. In order to avoid the overlap, the printing protocol needs to be adjusted such that the filaments and interconnects are all printed in a single pass. However, it was not possible to evaluate this in the Phase I program.

Resistive Interfilament Printing Demonstration. The ink jet printing was also tested to determine the feasibility of simultaneously printing the YBCO filaments interspaced with insulating filaments rather than spaces.

The printing of alternating YBCO and resistive filaments was demonstrated on one sample at MicroFab. The sample, shown in Figure 15, was prepared by first printing the YBCO filaments, then replacing the precursor ink and printing the resistive filaments on the second pass. In this initial demonstration there was no effort to optimize the widths of the individual filaments. In an actual manufacturing process the filaments would be printed simultaneously using a multi-nozzle print head. The samples were not processed to the final YBCO phase during the Phase I program.

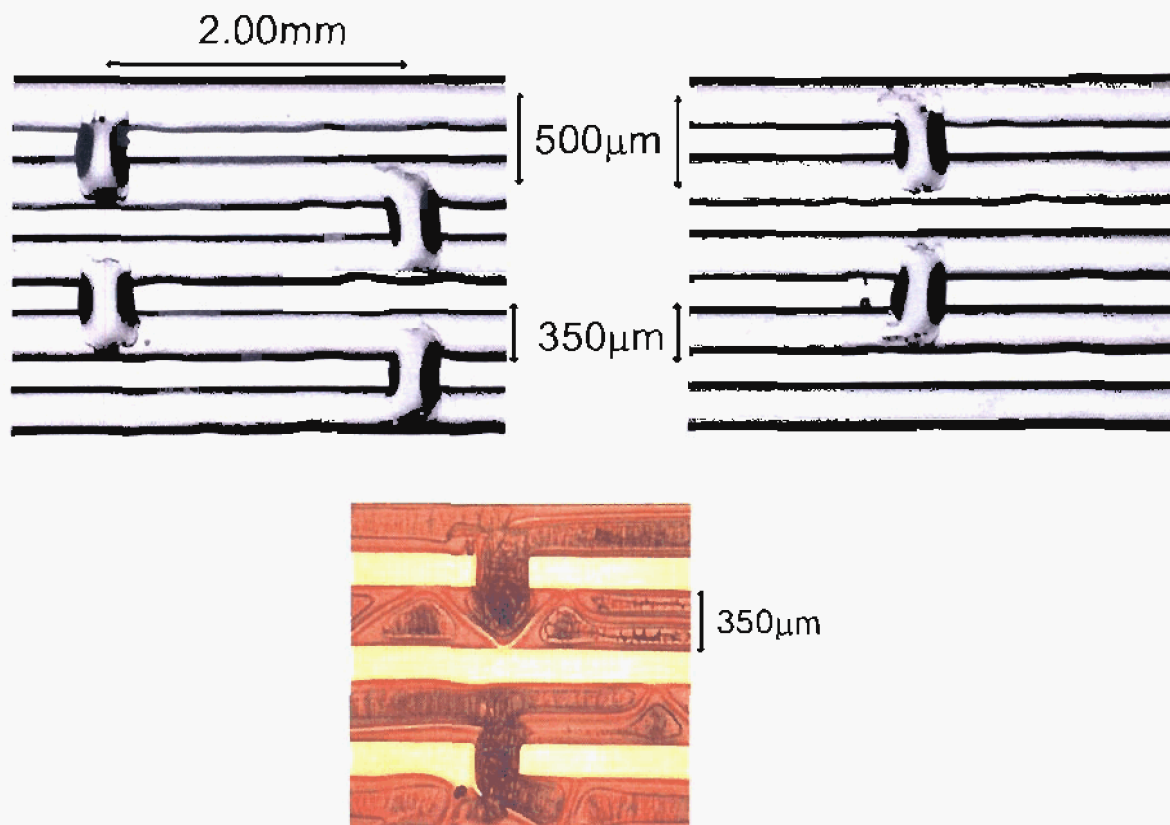


Fig. 14. Optical micrographs of 350 μm wide YBCO filaments ink jet printed with periodic interconnects. Top – “as printed”; Bottom – decomposed.

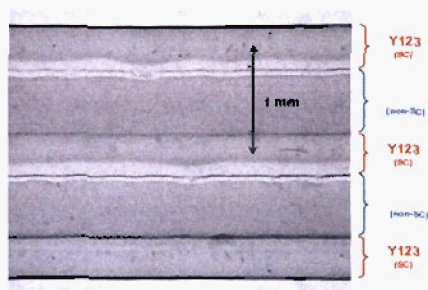


Fig. 15. Optical micrograph showing a series of alternating YBCO and resistive filaments ink jet printed on a RABiTS substrate.

Advanced Printing Optimization. A final print trial was carried out in June 2005. The goal was to demonstrate the printing of longer samples with filament widths of 200 μm to 4 mm as illustrated in Figure 16. These samples were to be used to optimization of the reaction conditions and to compare the I_c as a function of filament width. In addition the 4 mm wide samples would allow a direct comparison to the 4 mm conductors prepared by slitting the 4 cm strips in AMSC’s standard manufacturing process.

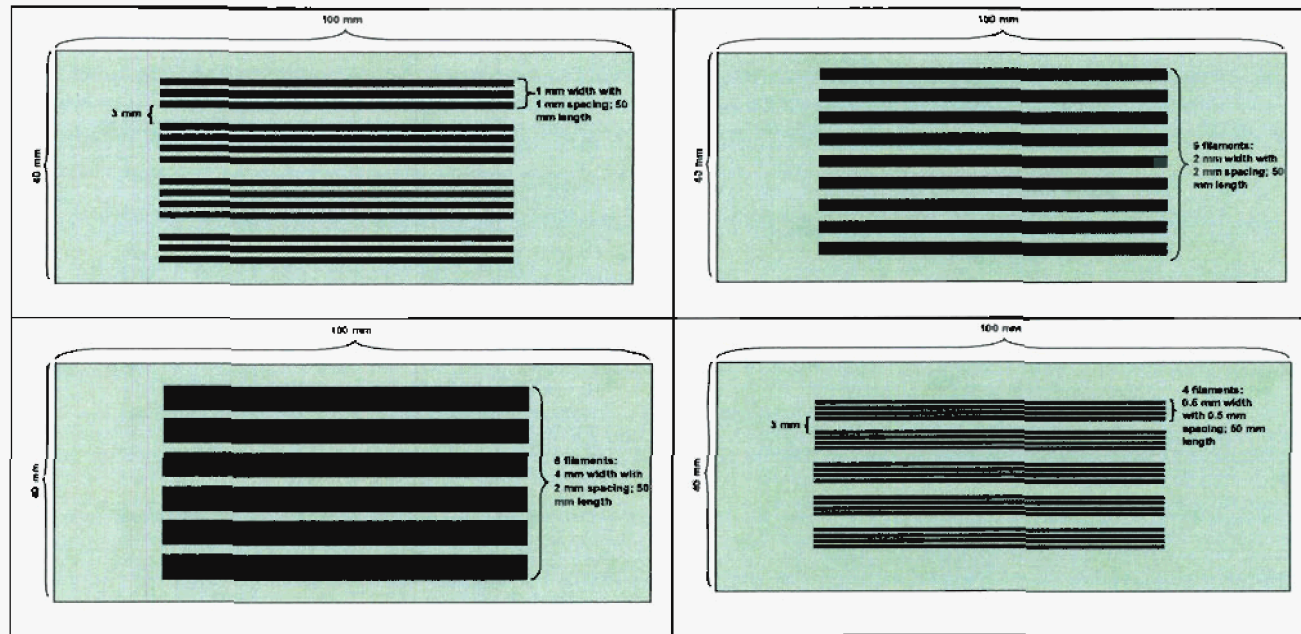


Fig. 16. Patterns of YBCO filaments printed in June 2005 printing trials at MicroFab Technologies, Inc.

In addition to the filament patterns shown in Figure 15, transposed filament architecture, shown in Figure 17, was tested. This transposed architecture has been developed and demonstrated under a separate STTR program for the development of ac conductors using a laser patterning technique [1]. However, the ability to directly print this architecture will allow a significant reduction in the manufacturing cost which will be required for development of commercial and military products.

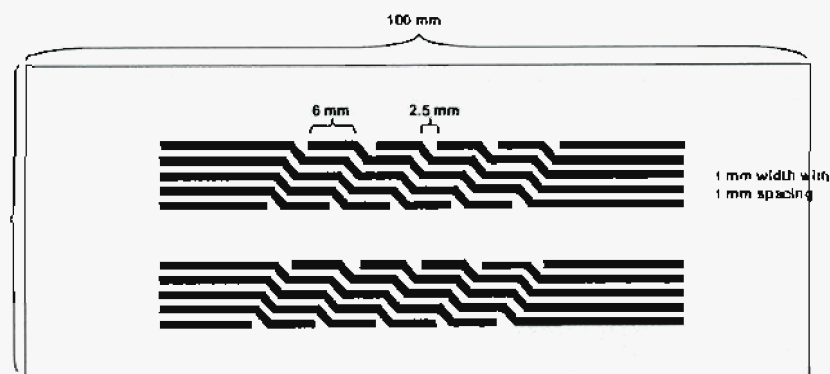


Fig. 17. Transposed YBCO filament architecture developed at AMSC for low loss ac-conductors. The filament architecture can be directly fabricated with the ink jet printing.

Task 3-a. Additional Task beyond Phase I SOW

The direct ink jet printing of a silver stabilizer layer on the YBCO filaments was also investigated during the Phase I program. The fabrication of practical, striated 2G wire for ac applications required the deposition of a metallic stabilizer layer on the individual YBCO as illustrated in Figure 18. In order to maintain the low ac loss in the striated conductors it is important that the stabilizer layer is not connected between filaments.

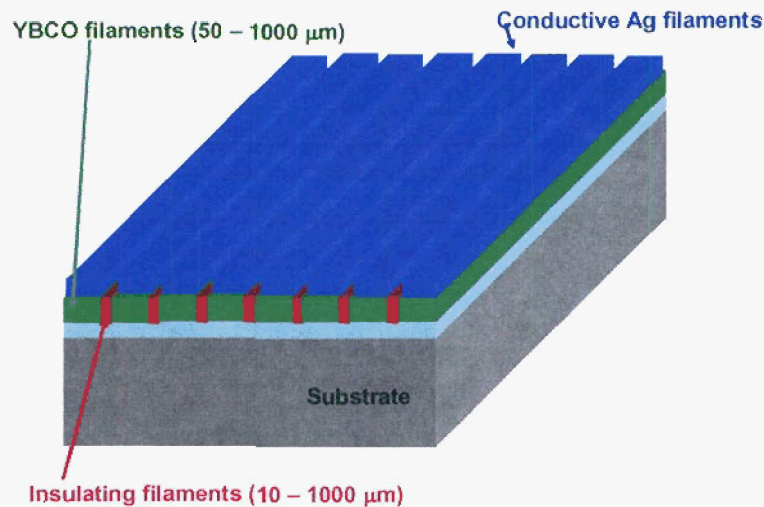


Fig. 18. Cross-sectional the YBCO/stabilizer architecture required for ac conductors made with striated YBCO filaments.

Ink jet printing of the stabilizer layer directly each individual YBCO filament is an effective low-cost process for manufacturing actual conductors. In fact, this approach has been developed for the deposition of 250 μm silver lines on ferrite filaments (Figure 19) that are also deposited by ink jet printing [14].

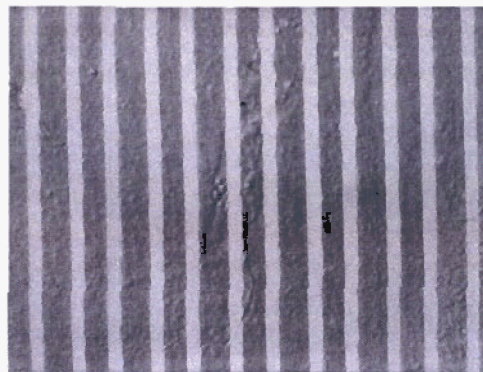


Fig. 19. Optical micrograph of 250 μm lines of silver nanoparticle ink printed onto a ferrite layer also deposited by ink jet printing [14].

The initial work in the Phase I program focused on selection a Ag ink, testing the compatibility of the Ag ink with the YBCO and demonstrating the ability to print the Ag onto the YBCO films.

The Ag ink, obtained from Cabot (AG-IJ-G-19=00-S1), is comprised of a Ag nanoparticle in a proprietary solvent [15]. The ink was designed for ink jet printing of high resolution, low resistivity Ag films for interconnects, bus bars, RFID's etc. The Ag is sintered at temperatures between 100 – 550°C, with the resistivity decreasing at higher temperatures,

To demonstrate the process, Ag films were directly ink jet printed on 1 cm x 2 cm areas of YBCO tapes and onto 500 μm wide YBCO filaments on RABiTS templates. The initial printing test showed that the surface condition of the YBCO affected the wetting of the ink on the YBCO film. However, pre-washing the YBCO with an alcohol based solvent prior to the ink jet printing of the Ag significantly improved the wetability allowing the formation of continuous Ag films as seen in Figure 20.

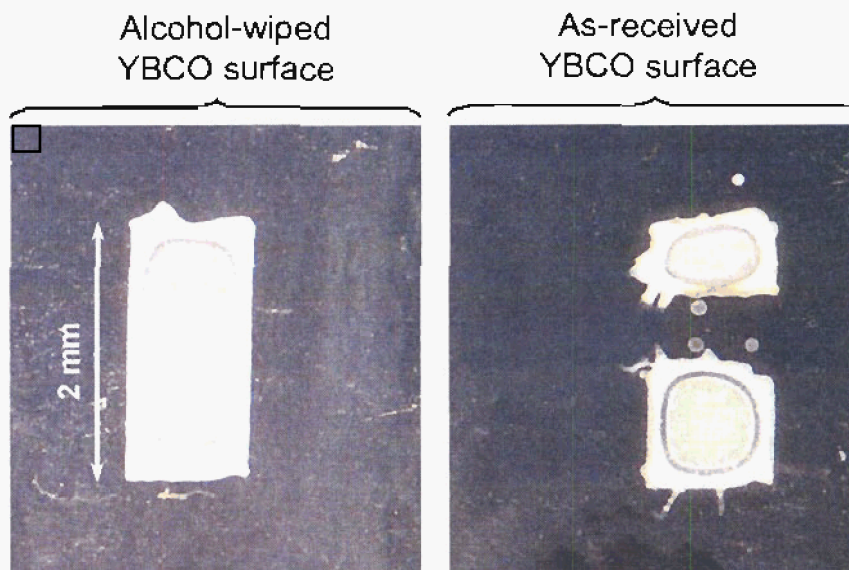


Fig. 20. Optical micrograph of 1 x 2 cm Ag films ink jet printed onto an alcohol cleaned YBCO film (left) and a YBCO film exposed to ambient atmosphere (right).

Figure 21 shows Ag layers printed on 500 μm wide striated YBCO filaments (YBCO striations were prepared by laser patterning). The Ag was deposited on the YBCO filaments at a width of 125, 175 and 325 μm . The standard print process produces a Ag thickness (after

sintering) of $0.4\text{ }\mu\text{m}$ per pass. Initial testing during the phase I program showed layers of $1.2\text{ }\mu\text{m}$ could be prepared by a 3 pass process.

YBCO bridges in films that coated with the $0.4\text{ }\mu\text{m}$ Ag ink layers showed essentially the same I_c as YBCO bridges coated with $1\text{ }\mu\text{m}$ thick sputtered Ag layers, again confirming that the Ag ink does not degrade the YBCO properties.

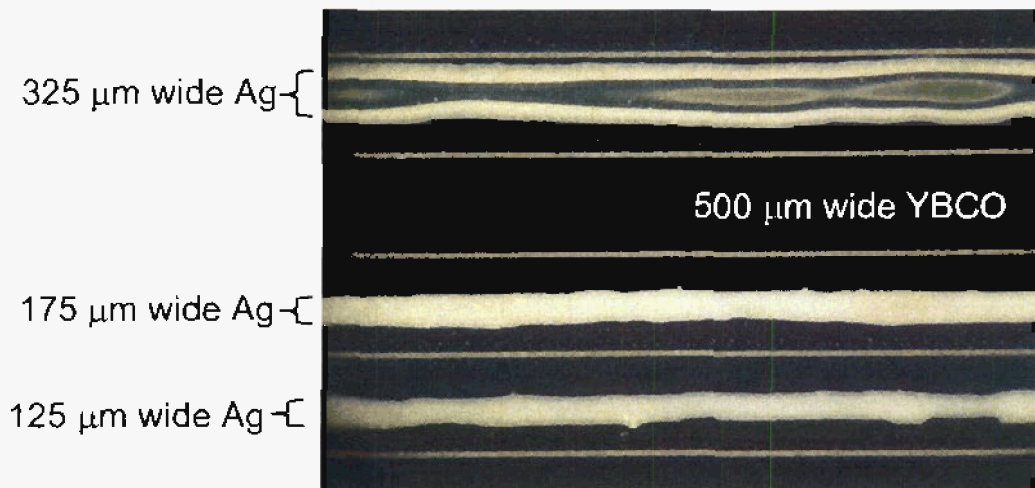


Fig. 21. Optical micrograph of 125, 175 and $325\text{ }\mu\text{m}$ wide Ag films printed on the surface of $500\text{ }\mu\text{m}$ wide YBCO filaments.

Task 4. Commercial Inkjet Design and Assessment.

Inkjet printing is a key technology which is enabling the rapid development of the direct writing technology across an expanding range of applications. The critical printer head technology used in ink jet printing has advanced significantly during the past few years and is currently being used in viable manufacturing solutions for numerous applications including low-cost, custom printing of a variety of functional material components such as ceramics, conductive polymers and metal oxides.

One of the major applications of direct printing is the manufacture of ceramic or metal oxide films that require the formation of discrete patterns. In conventional materials processing, the film is typically deposited by vacuum coating techniques, and thus covers the whole area of the substrate. Although this is useful in many applications, increasing numbers of applications, including the HTS tapes, require patterning the films to achieve specific properties or performance. Patterning the continuous layer is a time-consuming, costly, multi-stage process, involving lithographic masking and etching away of unwanted material or laser patterning to remove unwanted material. In contrast, the direct printing approach

provides a low-cost alternative method to manufacturing precisely patterned films over small or large area substrates.

The potential advantages of ink jet printing in manufacturing processes are evident from the current efforts to adapt it to a wide range of manufacturing operations including:

- **Electronic components and circuits:** flex circuits, RFID, PCB photomasks, wearable electronics, solar panels, fuel cells, batteries;
- **Flat Panel Display (FPD) Manufacture:** flat panel displays, PLED, LCD, color filters, display backplanes and flexible displays;
- **Chemical/Materials Development and Applications:** material development, substrate development and coatings;
- **3D Mechanical Applications:** 3D assembly systems and sensing;
- **Optical components:** optical lenses and light pipes;
- **Wide Format Graphics and Industrial Marking and Coding:** coding & marking, outdoor and indoor signage, point-of-sale displays, addressing and postal, decorative textiles, packaging, wall & floor coverings, commercial printing and screen masking.

The ink jet print heads that are currently being developed are designed for precision printing of complex patterns, high throughput, repeatability, reliability and low-cost.

The Phase I program focused on demonstrating that the ink jet printing process can be utilized for the deposition of striated YBCO filaments. The Phase I project used a single nozzle ink jet system to demonstrate the basic concept and process parameters. This single nozzle unit was capable of printing a 0.8 μm thick, 100 μm YBCO strip line at a rate of ~ 8 cm/sec. This translates to a rate of < 1 meter per hour for printing 60 individual 500 mm wide filaments across the width of a 4 cm wide RABiTS template.

The use of ink jet printing in a practical manufacturing process requires the use of a multi-jet print head. These types of print heads are used in many emerging materials applications. Typical, industrial print heads are designed with 125 to 256 individual nozzles that can be independently operated with print resolutions of 100 – 900 dpi. A typical print head available from Dimatrix, shown in Figure 22, has 256 nozzles and a resolution of 900 dpi. This type of print head would be capable of printing the entire width of a 4 cm substrate in a single pass. It is expected that rates in the range of meters per minute can be achieved, which is comparable to the current slot die coating processes used for the unstriated YBCO films. In

addition, since each nozzle can be independently controlled, this print head could be used to print YBCO and insulating filaments in a single pass.



Fig. 22. Photograph of an industrial piezoelectric ink jet print head available from Dimatrix. Print head has 256 independently controlled nozzles.

Incorporation of the industrial print heads into a reel to manufacturing process for the striated YBCO tapes requires development of a tape transport system that allows the precision placement of the ink along both the x-axis and y-axis as illustrated in Figure 23. In the design planned for Phase II, the pattern across the width of the substrate will be generated by controlling the printing of the individual nozzles. If necessary to achieve the resolution, the print head can also move slightly in the y-axis direction. The printing in the x-axis direction of the tape will be controlled by the movement of the tape from reel-to-reel. Developing the control of the translation of the tape in the x-axis will be an important aspect of the system design. The same printing system will also be used for the Ag printing on the striated YBCO filaments.

A major advantage of the ink jet printing process is that it can be readily inserted into the AMSC's existing baseline process. The RABiTS/MOD-YBCO manufacturing process used at AMSC is shown schematically in Figure 24. In the current baseline process, the YBCO film is deposited by a conventional slot die coating process. The ink jet print would simply replace the slot die system and not require any additional changes or additions to the 2G wire manufacturing process.

All in all, the ink jet process for the direct printing of patterned YBCO filaments for 2G HTS wire is assessed to have significant cost and performance advantages compared to conventional patterning approaches. Successful development of the ink jet printing process

will have a direct impact on the availability of low-cost 2G wire for military and commercial applications requiring low ac loss wire.

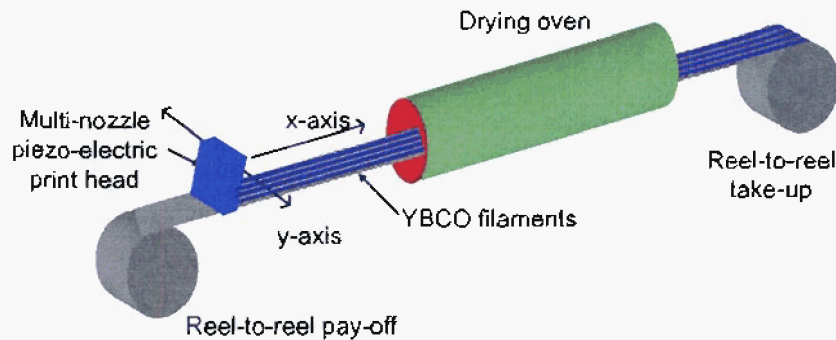
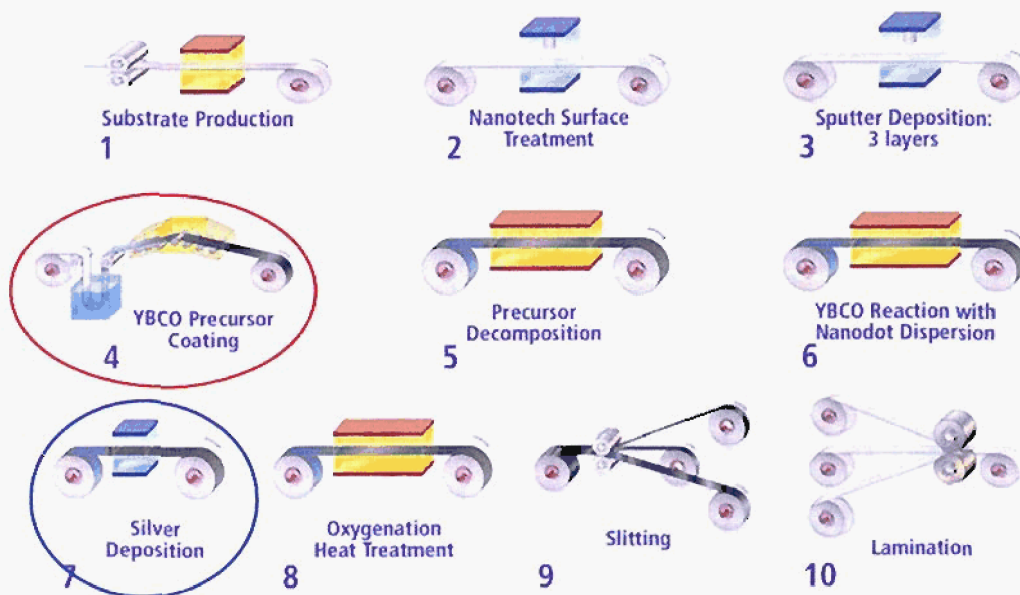


Fig. 23. Schematic of the proposed ink jet printing of striated YBCO filaments on a continuous RABiTS substrate.



3

Fig. 24. Schematic illustration of the 2G manufacturing process used at AMSC for fabrication of 2G wire by the RABiTS/MOD-YBCO process. The proposed ink jet print process for fabrication of striated YBCO filaments would replace the slot die coating process (red circle) used for the deposition of continuous YBCO films. The same ink jet print process would also replace the vacuum deposition (blue circle) of the Ag layer on the YBCO films. No other changes or additions to the manufacturing process are required to fabricate the patterned YBCO conductors.

REFERENCES

1. C. Thieme and O. Chevtchenko, "Novel 2G Conductor Design for AC Applications", Final Report, Office of Naval Research, Contract No: N00014-05-M-0050, August 2005.
2. S. Fleshler, M.W. Rupich and D. Verebelyi, Superconductivity for Electric Systems Annual Peer Review Washington, DC, August 2-4, 2005.
3. M.W. Rupich, U. Schoop, C.L.H. Thieme, D.T. Verebelyi, X. Li, W. Zhang, T. Kodenkandath, N. Nguyen, D. Buczek, E. Siegal J. Lynch, E. Thompson, B. Aldrich and J. Scudiere, "High Performance of 2G HTS Wire Based on a RABiTS™ Template and MOD YBCO Film" 106th American Society Meeting, Indianapolis, IN, April 18-21, 2004
4. M.W. Rupich, W. Zhang, X. Li, T. Kodenkandath, D.T. Verebelyi, U. Schoop, C. Thieme, M. Teplitsky, J. Lynch, N. Nguyen, E. Siegal, J. Scudiere, V. Maroni, K. Venkataraman, D. Miller, T. G. Holesinger, Physica C: Superconductivity, 412-414, Part 2, 7877-884 (2004).
5. M.W. Rupich, D. Verebelyi, C. Thieme, U. Schoop, X. Li, T. Kodenkandath, W. Zhang, M. Teplitsky, J. Scudiere, A. Goyal and M. Paranthaman "Development of 2G YBCO-RABiTS Wires," 2003 Annual Superconductivity Peer Review, Washington, DC, July 23-25, 2003.
6. M.W. Rupich, D. Verebelyi, C. Thieme, U. Schoop, X. Li, T. Kodenkandath, W. Zhang, M. Teplitsky, J. Scudiere, A. Goyal and M. Paranthaman "Development of 2G YBCO-RABiTS Wires," 2003 Annual Superconductivity Peer Review, Washington, DC, July 23-25, 2003.
7. P. C. McIntyre, M. J. Cima, A. Roshko, J. Appl. Phys. 77 (10) (1995), 5263.
8. P. C. McIntyre, M. J. Cima M.F. Ng, J. Appl. Phys. 68 (8) (1990), 4183.
9. J.A. Smith, M. J. Cima, M. N. Sonnenberg, IEEE Trans. Appl. Super. 9(2) (1999) 1531.
10. M. Rupich, Q. Li, S. Annavarapu, C. Thieme, W. Zhang, V. Prunier, M. Paranthaman, A. Goyal, D. F. Lee, E.D. Specht, and F. List, IEEE Trans. Appl. Superc. 11, 2927 (2001).
11. W.T. Norris, J. Phys. D3, 489 (1970).
12. E. Zeldov, J.R. Clem, M. McElfresh, and M. Darwin, Phys. Rev. B49, 9802 (1994).
13. C.E. Oberly, G.L. Rhoads, P.N. Barnes, L. Long, D.J. Scott, and W.J. Carr, Jr. Advances of Cryog. Engr. 48, 621 (2002).
14. <http://www.microfab.com/technology/energy/energy.html>
15. [http://www.cabot-corp.com/cws/businesses.nsf/8969ddd26dc8427385256c2c004dad01/dafbcd9206c1015187256f9b00025d82/\\$FILE/IJ P%20Ag%20Data%20Sheet.pdf](http://www.cabot-corp.com/cws/businesses.nsf/8969ddd26dc8427385256c2c004dad01/dafbcd9206c1015187256f9b00025d82/$FILE/IJ P%20Ag%20Data%20Sheet.pdf)